



Contents lists available at ScienceDirect

Life Sciences in Space Research

journal homepage: [www.elsevier.com/locate/lssr](http://www.elsevier.com/locate/lssr)

## EEG in extreme conditions: An advanced analysis pipeline for the human electroencephalographic signals recorded in space during the ALTEA experiment

Sara Sommariva<sup>a,\*</sup>, Giulia Romoli<sup>b</sup>, Elisabetta Vallarino<sup>a</sup>, Luca Di Fino<sup>b</sup>, Alberto Sorrentino<sup>a</sup>, Giorgia Santi Amantini<sup>b</sup>, Walter G. Sannita<sup>c</sup>, Michele Piana<sup>a</sup>, Livio Narici<sup>b</sup>

<sup>a</sup> Department of Mathematics, Università di Genova, Genoa, Italy

<sup>b</sup> Departments of Physics, Università di Roma Tor Vergata, Rome, Italy

<sup>c</sup> Department of Neurosciences, Rehabilitation, Ophthalmology, Genetics and Maternal and Infantile Sciences (DINO GMI), IRCCS San Martino, Università di Genova, Genoa, Italy

### ARTICLE INFO

MSC:  
00-01  
99-00

#### Keywords:

ALTEA project  
Long term mission  
EEG  
Impact cosmic radiation

### ABSTRACT

The Anomalous Long Term Effects in Astronauts (ALTEA) project originally aimed at disentangling the mechanisms behind astronauts' perception of light flashes. To this end, an experimental apparatus was set up in order to concurrently measure the tracks of cosmic radiation particles in the astronauts' head and the electroencephalographic (EEG) signals generated by their brain. So far, the ALTEA data set has never been analyzed with the broader intent to study possible interference between cosmic radiation and the brain, regardless of light flashes. The aim of this work is to define a pipeline to systematically pre-process the ALTEA EEG data. Compared to the analysis of standard EEG recording, this task is made more difficult by the presence of unconventional artifacts due to the extreme recording conditions that, in particular, require the EEG cap to be positioned next to another noisy electronic device, namely the particle detectors. Here we show how standard tools for the analysis of EEG data can be tuned to deal with these unconventional artifacts. After pre-processing the available data we were able to elucidate a shift of the center frequency of the  $\alpha$  rhythm induced by visual stimulation, thus proving the effectiveness of the implemented pipeline. This work represents the first study presenting results of signal processing of ALTEA EEG time series. Further, it is the starting point of a future work aimed at analyzing the interaction between EEG and cosmic radiation.

### 1. Introduction

Human exploration of deep space, starting with the return to the Moon, has raised the need for investigating and mitigating the effects on the astronauts' health of several space stressors, including cosmic radiation (Durante and Cucinotta, 2011; Cucinotta et al., 2014).

One of the documented side-effects of space travel is the astronauts' perception of phosphenes (light flashes) in the absence of any light sources. Studies correlating the perception of phosphenes to the local flux of charged particles (see the paper by Narici (2008), and references therein) suggested the action of ions on the eye retina or brain. Specifically, early studies on humans and recent studies on rodents or patients undergoing androtherapies in particles accelerator have documented a direct effect of the ions on both photoreceptor and neurons of the retina and suggested effects on the brain cortex (Carozzo et al., 2013, 2015; Sannita et al., 2006, 2007). However, the actual mechanisms causing the perception of these flashes upon exposure to charged particles

remain poorly understood. Altered vision, albeit only functional and transient, stands as a possible source of hazard in space and a concern for the astronauts' safety.

Direct electrophysiological measurements of the effect of cosmic radiation on the brain are lacking and the evidence remains inferential (Narici, 2008; Carozzo et al., 2013, 2015). The Anomalous Long Term Effects in Astronauts (ALTEA) (Narici, 2008) project has been specifically conceived to overfill this lack, i.e., to investigate the origin of light flashes with measurements in space. During the ALTEA project, a dedicated experimental facility has been built, which includes six identical particle detectors, a 32-channel electroencephalography (EEG) system, a visual stimulator, a push button, and a digital acquisition unit (Zaconte et al., 2010). This work concerns the data acquired through such a facility on the International Space Station (ISS) between August 2006 and July 2007.

\* Corresponding author.

E-mail address: [sommariva@dima.unige.it](mailto:sommariva@dima.unige.it) (S. Sommariva).

<https://doi.org/10.1016/j.lssr.2022.07.005>

Received 23 March 2022; Received in revised form 10 July 2022; Accepted 25 July 2022

Available online 29 July 2022

2214-5524/© 2022 The Committee on Space Research (COSPAR). Published by Elsevier B.V. This is an open access article under the CC BY-NC-ND license (<http://creativecommons.org/licenses/by-nc-nd/4.0/>).

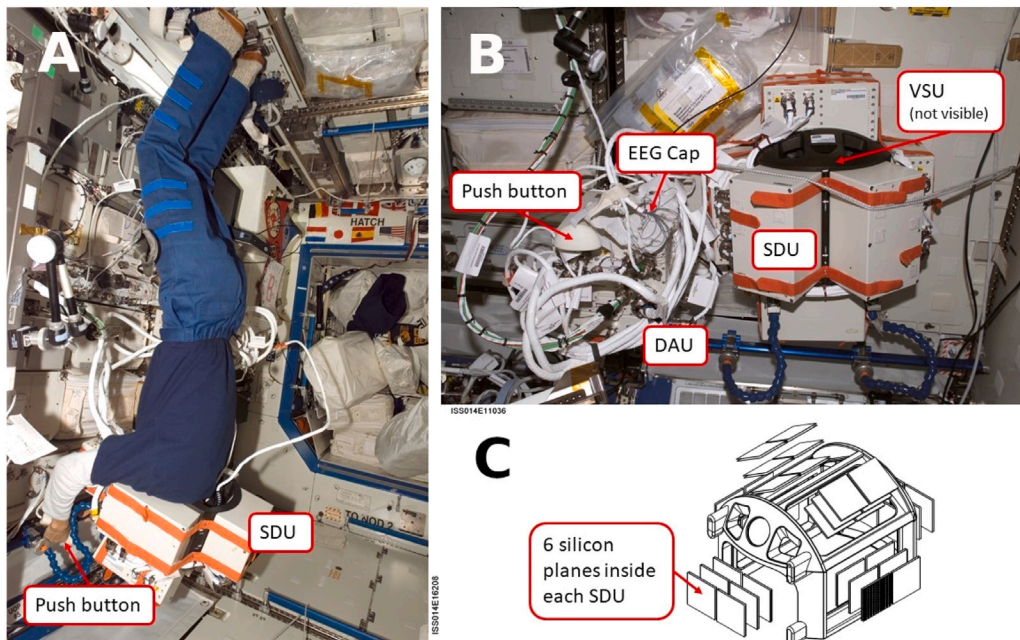


**Fig. 1.** ALTEA facility. (A) ALTEA helmet worn by one of the astronauts. (B) Whole ALTEA system on board the ISS. (C) Schematic representation of the 6 Silicon Detector Units (SDUs) highlighting the 6 panels that constitute each of them.

Results from a previous analysis of such a data set supported the hypothesis that cosmic radiation produces an electroretinogram (ERG) signal which is morphologically similar to the one measured after light stimulation (Narici, 2008). However, the ALTEA data set has never been analyzed with the broader intent to study possible interference between cosmic radiation and the brain, regardless of the light flashes perception. From this viewpoint, these are so far the only data where particles tracks in the astronauts' brain and eyes have been measured concurrently with astronauts' EEG signals.

Very few other EEG measurements in space have been conducted. Their main aim was to investigate the impact of microgravity on spontaneous brain oscillations, mostly  $\alpha$ , and their modulation in relation with a change of conditions from eyes open to eyes closed (Chéron et al., 2006; Leroy et al., 2007), and during a visuo-attentional task preceding a visuo-motor docking task (Cebolla et al., 2016). More recently, EEG measurements have been used to monitor sleep quality during space missions (Petit et al., 2019). However, all these experiments focused only on EEG and did not require other closed-by electrical apparatuses.

In this paper we thoroughly describe the pipeline we developed for preprocessing the ALTEA EEG data. Cleaning the ALTEA EEG data is a first, and peculiarly challenging step due to the fact that EEG sensors are positioned next to an advanced electronic device, namely the particle detector system, which generate unconventional artifacts in the recorded time series. Here, we will show how standard tools, such as finite impulse response (FIR) filters and Independent Component Analysis (ICA), can be used to suppress these unconventional artifacts. By applying this pipeline on the EEG time-series recorded aboard the ISS we were able to unravel a significant effect of trains of visual stimulation on the  $\alpha$  rhythm in orbit.

## 2. Experimental setup

### 2.1. The ALTEA facility

The ALTEA facility has been specifically devised to simultaneously detect astronauts brain activity and particles hitting their heads. To this end, the following units have been assembled (see Fig. 1).

- Six Silicon Detector Units (SDUs) for particle detection.

- A 32-channel EEG system.
- A Visual Stimulator Unit (VSU).
- A Digital Acquisition Unit (DAU).
- A push button.

The EEG system takes as input brain electrophysiological time series acquired via the cap in Fig. 2 and characterized by 28 specifically designed gel sensors among which 26 monopolar sensors monitor the brain activity and 2 bipolar sensors record the electroretinogram. In order to sync the EEG signal with particle data, DAU injects a sync signal in one EEG channel. This induces a peculiar spike in the EEG recordings that needs to be removed as described in Section 3.

### 2.2. The EEG acquisition paradigm

The data cohort was made of seven sessions, each one of about 90 min, i.e., approximately the orbit time. As detailed in Table 1, the ALTEA experiment on board the ISS involved three astronauts, from now on denoted as sub01, sub02, and sub03. The stimulation paradigm is described in Fig. 3 and is made of three phases:

- *stim 1* phase (8 min): gray scaled vertical bars at different spatial frequencies and contrast.
- *stim 2* phase (22 min, 12 trains spaced with inter-train intervals of about 84 s): 156 point-like visual stimulations, 112 in the upper left corner and 48 in the lower right corner.
- *resting* phase ( $58 \pm 21$  min, average and standard deviation over sessions): light flashes needed to be reported by pressing the push button.

This same visual stimulation paradigm was utilized for data acquisition at ground, prior to the mission, from the same subjects. In the remaining of this work only the *stim 2* and the resting phases will be considered.

## 3. Data processing pipeline

This section describes the pipeline we developed for pre-processing the ALTEA EEG data from the sessions reported in Table 1. The figures

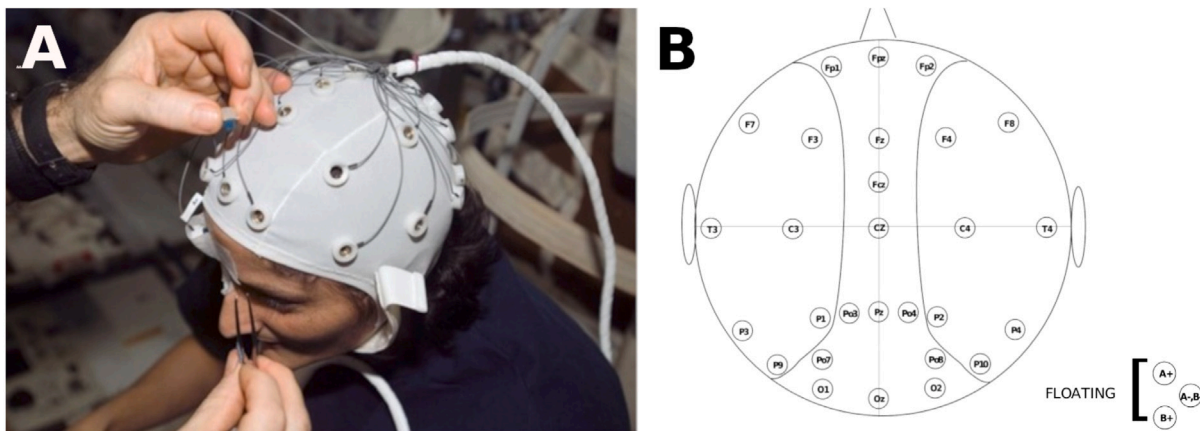


Fig. 2. The EEG cap worn by one of the astronauts (A), and corresponding sensors montage (B).

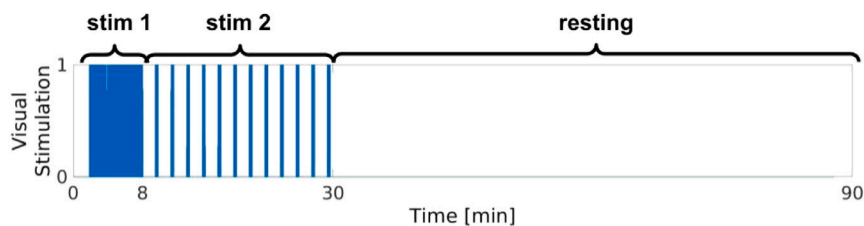


Fig. 3. Acquisition paradigm for the EEG experiments. Blue vertical lines identify the time intervals during which trains of visual stimulations were delivered to the astronauts. Based on the stimulation rate, each recording session was split in three phases (stim 1, stim 2, and resting).

Table 1

Number and duration of the recording sessions performed by each one of the three astronauts involved in the ALTEA experiment on board the ISS.

Astronaut	Sub01	Sub02			Sub03		
No. of sessions	1	4			2		
Duration [min]	88	95	93	117	92	48	91

refer to one session, namely the resting phase of sub01's recording session, which we considered to be as the most representative.

A schematic illustration of the pipeline is given in Fig. 4, where the operational steps are in the blue boxes and the corresponding mathematical implementation is given in red. From a computational viewpoint, we have used both routines implemented in EEGLAB (Delorme and Makeig, 2004) and customized MATLAB® functions. Additionally, we adapted a plotting routine from FieldTrip (Oostenveld et al., 2011) in order to visualize the time-series.

Following an integrity check of the data (see Appendix for more details), the first pre-processing step is the application of a high-pass filter with low-frequency cut-off equal to 1 Hz, since slow baseline changes are unreliable due to high noise level associated to the peculiar experimental setting. Then we applied a low-pass filter with high-frequency cut-off equal to 45 Hz to suppress high-frequency noise components. The [1,45] Hz filtering is typical for the processing of physiological signals (Jas et al., 2018) and has been obtained by using the Finite Impulse Response (FIR) filter implemented in EEGLAB.

As shown in Fig. 5 ALTEA EEG data are characterized by two kinds of artifacts associated to malfunctioning of specific EEG channels and to the presence of the sync signal from the DAU.

In these difficult experimental conditions, sensors' malfunctioning is a consequence of a non optimal contact of the electrode on the skull and, as can be seen in Fig. 6, it results in an abnormally high spectrum of the corresponding signals. Motivated by this consideration, malfunctioning channels have been selected by computing for each sensor the norm of the Power Spectrum of the recorded signal over

frequencies greater than 13 Hz. This value has been chosen so to avoid the frequency band associated to the  $\alpha$  rhythm, where sensors over the occipital lobe obviously present a greater power than the other sensors. For each sensor, the power spectrum is computed by using the Welch's method (Welch, 1967; Vallarino et al., 2021) with an Hamming window applied to non-overlapping segments of 8 sec in order to obtain a frequency resolution of 0.125 Hz. As illustrated in Fig. 6, channels showing a value of the computed norm significantly higher (more than one standard deviation) than the mean value over sensors are removed from the analysis.

Artifacts associated to sync signal from the DAU are removed by means of a computational approach based on Independent Component Analysis (ICA). To this end, for each session the ICA decomposition of the corresponding EEG time-series has been computed using EEGLAB implementation of the *infomax* algorithm (Makeig et al., 1997). As illustrated in Fig. 7 for the representative subject, each session shows a group of independent components with similar spatial pattern and whose time-courses were characterized by the 1 Hz spikes of the sync signal. Such artifactual components were rejected by visual inspecting the results of ICA decomposition.

Downstream from the artifacts removal, the pipeline computes the power spectrum. The presence of possible additional bad channels is pointed out in the power spectrum by using the same approach as in the time series, i.e., computing the norm of the power spectrum and removing those sensors presenting a significant higher values with respect to the distribution over all channels.

The described pipeline was used to separately preprocess the stim 2 and the resting phases of all the seven available recording sessions.

## 4. Results

### 4.1. Outcome of the preprocessing

Fig. 8, top row, shows, in both frequency and time domains, an example of raw recording corresponding to resting phase for one of the sessions acquired from sub01. The effects of both the presence

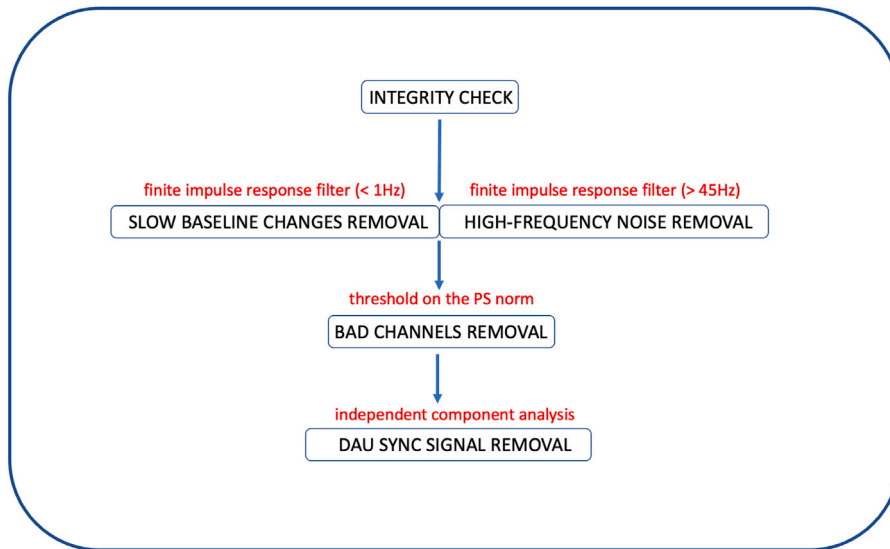


Fig. 4. The ALTEA pre-processing pipeline. Blue boxes report the operational steps that constitute the pipeline while their mathematical implementation is described in the above red text. PS: Power Spectrum.

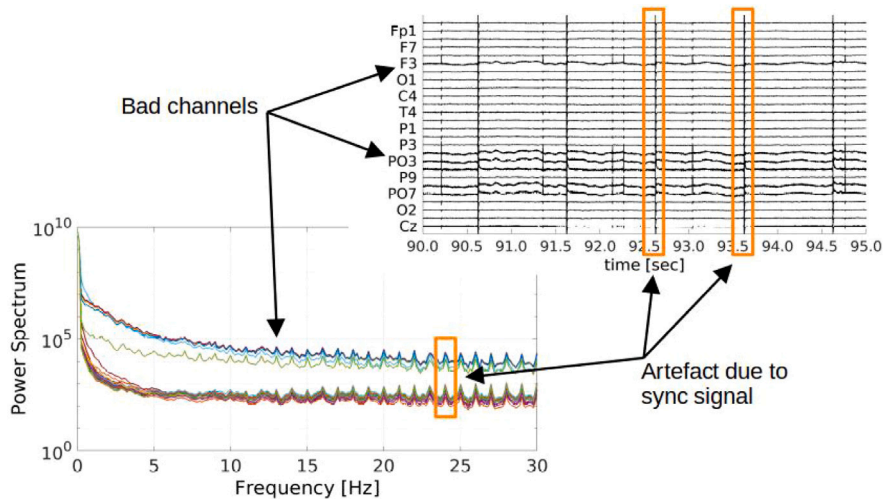


Fig. 5. ALTEA-specific artifacts in the EEG data, visible both from the EEG time-series (upper, right panel) and from the corresponding power spectrum (lower, left panel).

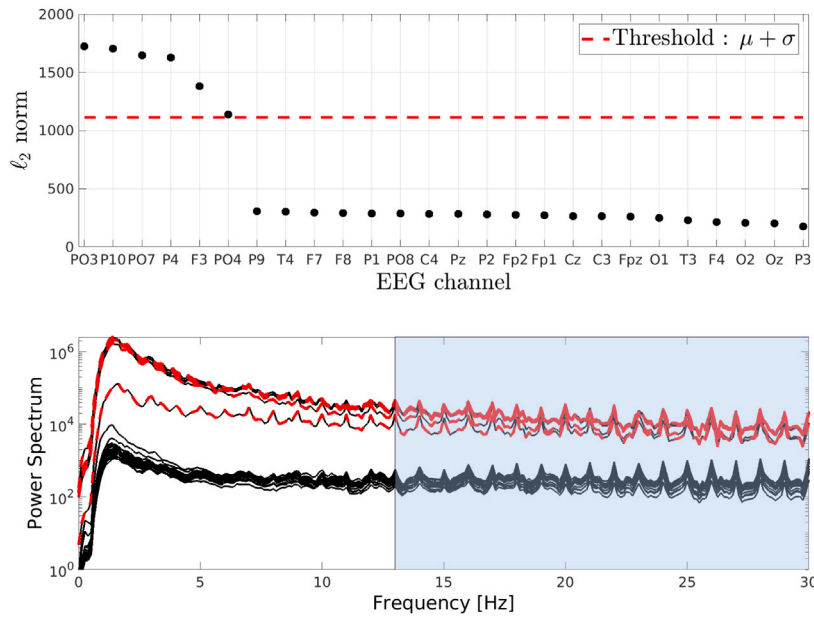
of malfunctioning sensors and spikes related to the DAU sync signal are clearly visible and, for example, completely mask the existence of the  $\alpha$  rhythm. Downstream the application of the pre-processing pipeline, in Fig. 8, bottom row, this  $\alpha$  oscillation clearly stands out from the background signal at around 10 Hz. The elimination of the DAU sync signal and of the effects of malfunctioning sensors is pursued also in the other two subjects, thus making these data usable for neurophysiological considerations.

#### 4.2. Impact of stimulation on the $\alpha$ rhythm

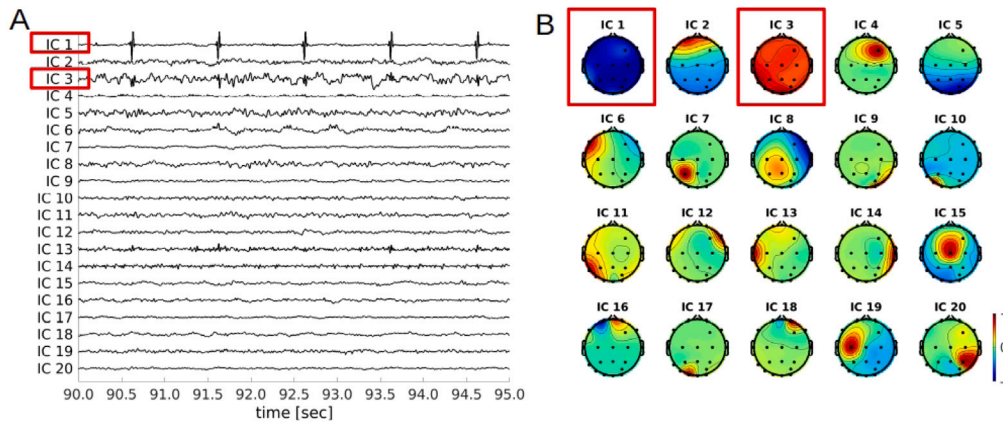
Starting from the data processed by means of the pipeline summarized in Fig. 4, for each recording session we computed the power spectrum of the time-series acquired during the resting phase and of the time-series corresponding to the intervals between the different trains of stimulation in the stim 2 phase. To extract such intervals, we selected, for each of the 12 inter-train intervals, eight consecutive non-overlapping segments of 8 sec, starting 16 sec after the last trigger of each train of stimulation. The power spectrum was then computed by means of the Welch's method with Hamming window.

Fig. 9 shows the result for one representative session performed by sub02. The power spectrum computed from all the four recording sessions involving this subject present a double peak in the frequency band characteristic of the  $\alpha$  rhythm, i.e., [6, 11] Hz. These two maxima show up in the power spectrum of both the resting phase and the inter-train intervals of the stim 2 phase. However, in the inter-train case (bottom row of the figure) the peak at higher frequency is shifted toward left. This behavior is coherent with previous results obtained in studies on the impact of train of stimulation on brain rhythms performed in on-Earth laboratories by using a magnetoencephalography (MEG) data set (Narici and Peresson, 1995).

To quantify such a shift in Fig. 10 we show mean and standard deviation over the four sessions involving sub02 of the center frequencies where the peaks occur. To compute the values of the center frequencies we only considered the sensors over the posterior and occipital lobes, i.e., referring to the montage in Fig. 2, those starting with letters *P* and *O*. While the slower peak was around 8 Hz both in the resting and the inter-train condition, the second peak shifted from about 10.12 Hz to 9.56 Hz.



**Fig. 6.** Automatic detection of the malfunctioning channels. Upper panel: norm of the Power Spectra over the frequency bands [13,45] Hz of the recorded EEG time-series. The red dotted line represents the threshold used to select the malfunctioning channels.  $\mu$  and  $\sigma$  stand for average and standard deviation over sensors, respectively. Lower panel: amplitude of the Power Spectrum of the EEG data. Selected malfunctioning channels are marked in red, while the blue area represents the frequency band used to compute the norm in the upper panel. The plot has been cut at 30 Hz for visualization purpose.



**Fig. 7.** (A) Five seconds of activation of the independent components computed from the resting phase of one representative recording session, and (B) corresponding scalp topographical maps. Red boxes highlight the components that have been removed because responsible for the artifact related to the DAU sync signal.

#### 4.3. Comparison with on-Earth acquisitions

For sub02 we have at disposal an EEG recording acquired on Earth prior the ALTEA mission, while the subject was performing the visual stimulation tasks (phase stim 1 and stim 2 of the EEG paradigm depicted in Fig. 3). A visual inspection of the data revealed that no malfunctioning sensors were present in the data. Moreover, since the particle detector units were turned off during on-Earth acquisition, there was no need to remove the characteristic spiky artifact affecting data acquired on-board. For these reasons, to process the EEG time series acquired on Earth we limited the pipeline of Fig. 4 to the band-pass filter in [1,45] Hz implemented as described in Section 3. We then computed the power spectrum of the inter-train intervals of the stim 2 phase extracted as described in the previous subsection. As it can be seen from Fig. 11 similarly to what has been described in the previous section, also for the on-Earth acquisition the power spectrum of the time-series acquired by posterior and occipital sensors presented two peaks in the  $\alpha$  frequency band. The center frequencies of such peaks are at 8 Hz and 9.12 Hz, respectively.

#### 5. Discussion

Minimizing health risks during deep space voyages is of paramount importance in planning human space exploration missions. The possible interaction between the combination of space hazards and brain function is now considered one of the major concerns in deep space flight.

The only relevant tool available in space to monitor brain physiology is EEG. However, the usability and reliability of EEG measurements in space have been often questioned, due to the very peculiar situation in which the data are acquired.

In order to successfully operate an EEG in space it is therefore mandatory either to configure the experiment in the cleanest possible way, measuring EEG far from any other electronic apparatus, or to be able to proficiently face the extra noise and extract useful information even from noisy EEG tracks acquired in these extreme conditions.

Radiation is one of the main health hazards in space, and the set of EEG data presented in this paper is unique as it is acquired in concurrence of data about particles impinging in the brain. This very

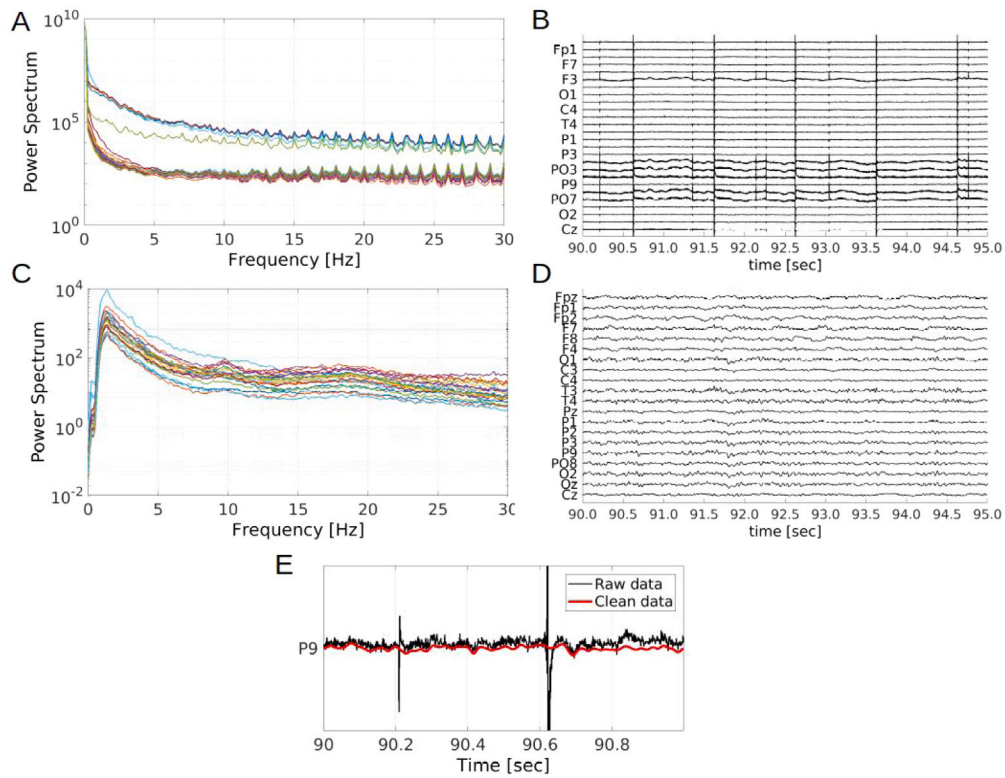


**Fig. 8.** Original (A–B) and preprocessed data (C–D) corresponding to the resting phase of one representative recording session. Panels (B) and (D) show the EEG time-courses while panel (A) and (C) display the corresponding power spectra in logarithmic scale. For visualization purposes, original and preprocessed time series are plotted with different scales and only a subset of the channel labels are reported in panel (B). For a better comparison, panel (E) shows 1 s of the original (raw) and preprocessed (clean) data corresponding to the occipital channel P9 plotted with the same scale.

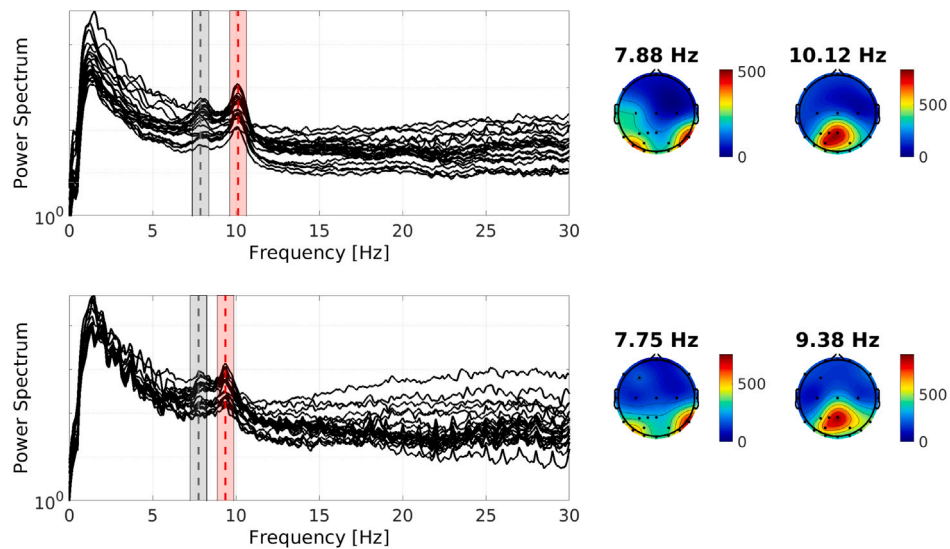


**Fig. 9.** Power spectrum of the time-series recorded during the resting phase (upper row) and the inter-train intervals of the stim 2 phase (lower row) for one representative session of sub02. The gray and red bar show a 1 Hz interval centered in the two peaks that clearly show up in the  $\alpha$ -band. The averaged value of the cross-power spectrum on these two frequency bands is plotted in the scalp topographical maps on the right. The center frequency for each one of the peaks is shown above the topographical maps.



Fig. 10. Center frequencies of the two peaks characterizing sub02's power spectra. The error bars have been obtained by computing mean and standard deviation of the results across the four sessions performed by sub02 considering the resting phase (blue) and the inter-train intervals of the stim 2 phase (red).

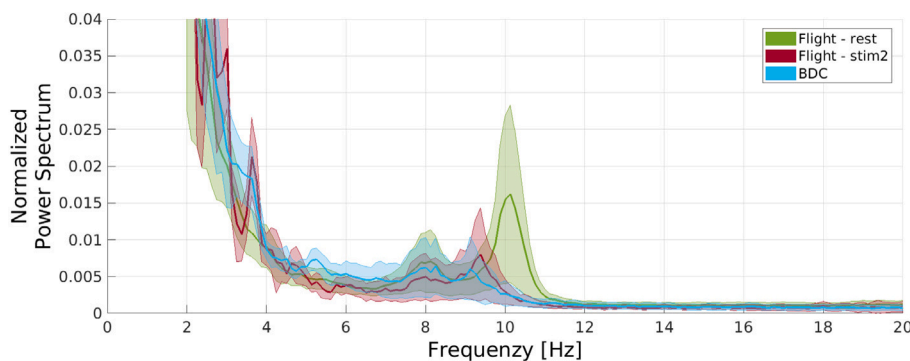


Fig. 11. Comparison of the Power Spectra of the EEG time-series recorded on Earth (BDC, Baseline Data Collection) and that corresponding to the resting phase and the inter-train intervals of the stim2 phase of one acquisition session on board the ISS performed by sub02. Each colored band represents the mean and the 1 standard deviation confidence interval obtained by averaging the power spectra of the posterior-occipital sensors each one normalized by the corresponding norm.

special experimental configuration brings a high performance particle detector quite close to the EEG electrodes, with the inevitable increase in noise and artifacts. Even if this configuration is unique, the noise and the artifacts may well mimic noise and artifacts that could be found in space under different experimental conditions.

Therefore, in the process for analyzing the possible interactions of the EEG with radiation, we were faced with the problem of cleaning the data in a suitable way to proceed with the cross analysis with the particle data. As mentioned above, the data cleaning solution proposed here could be used also under similar, but different, configurations.

In this paper we presented the pipeline for this cleaning procedure and its validation. Although the proposed pipeline is based on standard tools of EEG data analysis, such as Independent Component Analysis, the way in which such tools are applied to our data is completely unconventional and tailored to the specific artifacts arising in the EEG acquisition in space. The resulting cleaned data showed electrophysiological behaviors already evidenced on ground: the slowing of the  $\alpha$  rhythm in proximity of a series of stimulation. This is a double result: i) it validates the proposed cleaning pipeline, and (ii) it also demonstrates that this specific  $\alpha$  rhythm behavior is the same even in microgravity, and under all the space stressors.

This study describes the first analysis of EEG data acquired in space during the ALTEA experiment. The cleaning pipeline developed for this study together with the results of the analysis are the starting point for a more thorough study concerning the interaction between cosmic radiation and astronauts' neurophysiological response. The study of such an interaction is made more difficult by the need to distinguish between alterations in the neurophysiological response actually related to cosmic radiation from those induced by other confounding space

stressors. To overcome this issue, on the one hand we plan to use powerful statistical tools to identify truly significant events. On the other hand, we will exploit a set of EEG recordings acquired on Earth while the astronauts were performing the same visual stimulation task performed on-board the ISS. These data will allow us to disentangle systematic changes in the astronauts' brain activity due to confounding space stressors from those related to cosmic radiation. Specifically, we expect the latter to occur only at specific time-points corresponding to the instants of impact of the particles, and to induce a response of the visual system with a time-scale and a morphological pattern similar to that of visual evoked potentials.

#### Declaration of competing interest

The authors declare that they have no known competing financial interests or personal relationships that could have appeared to influence the work reported in this paper.

#### Funding

The financial support of the "ALTEA Brain Rad" ASI grant n. 2018-1S-HH.O is kindly acknowledged.

#### Appendix. Integrity check on data

During the Central Nervous System Monitoring (CNSM) configuration of the ALTEA facility, EEG data have been stored in the form of Express Rack Telemetry packets (Di Fino et al., 2006). Each packet contains 16 time-points of EEG data acquired at 1024 Hz together with a

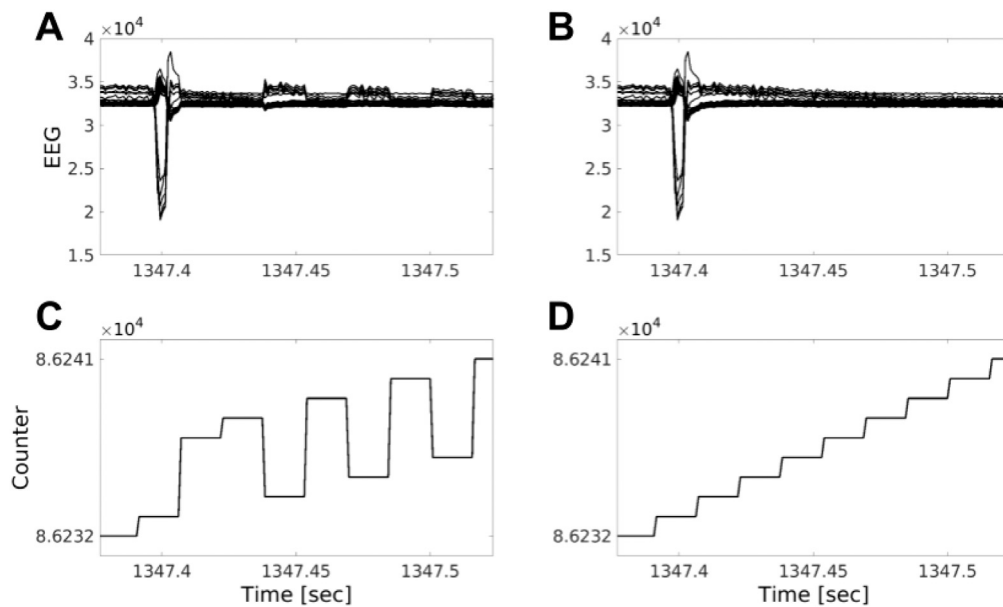


Fig. A.12. Raw EEG data and counter before (left panels) and after (right panels) correcting the temporal axis. Panel A and B shows 150 ms of sub01's recording session, while panel C and E represent the value of the counter in the corresponding Express Rack Telemetry packets.

counter and a time-tag representing the order and time of acquisition of the packet, respectively. In a preliminary integrity check of the data, we used time-tag and counter to verify that the complete EEG recordings were correctly transmitted to ground. Due to errors in the storing order of Express Rack Telemetry packets, all EEG recording presented some discontinuities similar to those shown in Fig. A.12. This issue has been fixed by simply reordering the temporal axis so to obtain not decreasing values of the counter as in panel D of Fig. A.12.

## References

- Carozzo, S., Ball, S.L., Narici, L., Schardt, D., Sannita, W.G., 2015. Interaction of  $^{12}\text{C}$  ions with the mouse retinal response to light. *Neurosci. Lett.* 598, 36–40.
- Carozzo, S., Narici, L., Schardt, D., Combs, S., Debus, J., Sannita, W., 2013. Electrophysiological monitoring in patients with tumors of the skull base treated by  $^{12}\text{C}$  radiotherapy. *Int. J. Radiat. Oncol. Biol. Phys.* 85, 978–983.
- Cebolla, A.M., Petieau, M., Dan, B., Balazs, L., McIntyre, J., Chéron, G., 2016. Cerebellar contribution to visuo-attentional alpha rhythm: insights from weightlessness. *Sci. Rep.* 6 (1), 1–10.
- Chéron, G., Leroy, A., De Saedeleer, C., Bengoetxea, A., Lipshits, M., Cebolla, A., Servais, L., Dan, B., Berthoz, A., McIntyre, J., 2006. Effect of gravity on human spontaneous 10-hz electroencephalographic oscillations during the arrest reaction. *Brain Res.* 1121 (1), 104–116.
- Cucinotta, F.A., Alp, M., Sulzman, F.M., Wang, M., 2014. Space radiation risks to the central nervous system. *Life Sci. Space Res.* 2, 54–69.
- Delorme, A., Makeig, S., 2004. Eeglab: an open source toolbox for analysis of single-trial eeg dynamics including independent component analysis. *J. Neurosci. Methods* 134 (1), 9–21.
- Di Fino, L., Belli, F., Bidoli, V., Casolino, M., Narici, L., Picozza, P., Rinaldi, A., Ruggieri, D., Zaconté, V., Carozzo, S., et al., 2006. Altea data handling. *Adv. Space Res.* 37 (9), 1710–1715.
- Durante, M., Cucinotta, F.A., 2011. Physical basis of radiation protection in space travel. *Rev. Modern Phys.* 83 (4), 1245.
- Jas, M., Larson, E., Engemann, D.A., Leppäkangas, J., Taulu, S., Hämäläinen, M., Gramfort, A., 2018. A reproducible MEG/EEG group study with the MNE software: recommendations, quality assessments, and good practices. *Front. Neurosci.* 12, 530.
- Leroy, A., De Saedeleer, C., Bengoetxea, A., Cebolla, A., Leurs, F., Dan, B., Berthoz, A., McIntyre, J., Cheron, G., 2007. Mu and alpha EEG rhythms during the arrest reaction in microgravity. *Microgravity Sci. Technol.* 19 (5), 102–107.
- Makeig, S., Jung, T.-P., Bell, A.J., Ghahremani, D., Sejnowski, T.J., 1997. Blind separation of auditory event-related brain responses into independent components. *Proc. Natl. Acad. Sci.* 94 (20), 10979–10984.
- Narici, L., 2008. Heavy ions light flashes and brain functions: recent observations at accelerators and in spaceflight. *New J. Phys.* 10 (7), 075010.
- Narici, L., Peresson, M., 1995. Discrimination and study of rhythmical brain activities in the  $\alpha$  band: a neuromagnetic frequency responsiveness test. *Brain Res.* 703 (1–2), 31–44.
- Oostenveld, R., Fries, P., Maris, E., Schoffelen, J.-M., 2011. Fieldtrip: open source software for advanced analysis of MEG, EEG, and invasive electrophysiological data. *Comput. Intell. Neurosci.* 2011.
- Petit, G., Cebolla, A.M., Fattinger, S., Petieau, M., Summerer, L., Cheron, G., Huber, R., 2019. Local sleep-like events during wakefulness and their relationship to decreased alertness in astronauts on ISS. *Npj Microgravity* 5 (1), 1–9.
- Sannita, W., Ball, S., Belli, F., Bidoli, V., Carozzo, S., Casolino, M., Di Fino, L., Peachey, N., Picozza, P., Pignatelli, V., et al., 2007. Implications for human space travel of mice retinal responses to  $^{12}\text{C}$  ions. *Neurosci. Lett.* 416, 231–235.
- Sannita, W.G., Narici, L., Picozza, P., 2006. Positive visual phenomena in space: A scientific case and a safety issue in space travel. *Vis. Res.* 46 (14), 2159–2165.
- Vallarino, E., Sorrentino, A., Piana, M., Sommariva, S., 2021. The role of spectral complexity in connectivity estimation. *Axioms* 10 (1), 35.
- Welch, P., 1967. The use of fast Fourier transform for the estimation of power spectra: a method based on time averaging over short, modified periodograms. *IEEE Trans. Audio Electroacoust.* 15 (2), 70–73.
- Zaconté, V., Casolino, M., Di Fino, L., La Tessa, C., Larosa, M., Narici, L., Picozza, P., 2010. High energy radiation fluences in the ISS-USlab: ion discrimination and particle abundances. *Radiat. Meas.* 45 (2), 168–172.